

# HIGH-THROUGHPUT ANALYSIS OF NUCLEOSIDE- AND NUCLEOTIDE-BINDING BY PROTEINS

JUSTIN K.M. ROBERTS<sup>1\*</sup>, CECELIA WEBSTER<sup>1</sup>,  
THOMAS C. TERWILLIGER<sup>2</sup> AND CHANG-YUB KIM<sup>2</sup>

<sup>1</sup>Department of Biochemistry, University of California,  
Riverside, CA 92521, USA.

<sup>2</sup>Bioscience Division, MS M888, Los Alamos National Laboratory,  
Los Alamos, NM 87545, USA.

**E-Mail:** [\\*justin.roberts@ucr.edu](mailto:justin.roberts@ucr.edu)

*Received: 25<sup>th</sup> June 2008 / Published: 16<sup>th</sup> March 2009*

## ABSTRACT

Many proteins function via selective binding of small molecules, and an important class of ligands is nucleosides, including derivative mono- and dinucleotides, which participate in processes such as catalysis and signal transduction. Determining the specificity of nucleoside/nucleotide binding is therefore central to understanding the function of many proteins. We describe use of dye-ligand affinity chromatography methods to identify putative nucleotide-binding proteins, and to determine the specificity of binding to structurally related ligands. In one approach, putative nucleoside-binding proteins are captured from crude protein extracts of cells, for identification via standard proteomic methods. In a second approach, interactions of different nucleosides with purified recombinant protein targets, immobilized on dye, are determined to assess the specificity of ligand recognition by a given nucleotide-binding protein in the context of structural and functional genomics, and drug development.

## INTRODUCTION

Nucleosides and their derivatives are molecular carriers central to transmission of energy, genetic information and intracellular signals, serving in these roles usually via specific interactions with proteins [1]. Furthermore, many drugs contain nucleoside-related moieties; for example nucleotide-protein interactions are considered critical in the action of isoniazid, one of the most efficient drugs for the treatment of *Mycobacterium tuberculosis* (Mtb) infections [2] and purine nucleoside analogs have been recently developed as anti-Mtb drug candidates [3]. Identification of protein-nucleoside ligand couples, and understanding the basis for functional molecular interactions, are complicated by obscurities in the relationships between gene sequences and ligand binding specificity. For example, enzymes sharing sequence similarity can exhibit differences in nucleotide specificity [4–6], and the specific ligand-binding properties of individual proteins can be sensitive to small changes in gene sequence [7–9]. Aiming to complement bioinformatics approaches to protein function [10, 11], we describe a biochemical screen based on dye-ligand chromatography [12] that can be used to obtain evidence for specific protein-ligand interactions and to assess selectivity of protein-ligand interactions in the human pathogen *Mycobacterium tuberculosis*.

Affinity binding technologies provide a means to identify physical interactions between macromolecules and their small-molecule partners [13–15]. The technique of dye-ligand chromatography has been used to purify a wide variety of proteins [12]. Cibacron Blue F3GA binds many nucleoside-dependent enzymes and, by selective elution with salt or ligands such as NADH or AMP, these proteins can often be purified [12]. Here we use the selective elution of proteins from F3GA chromatography resin as a high-throughput assay for protein-ligand interactions. The premise in our approach is that if a ligand can trigger release of a protein adsorbed on the dye-column, the ligand probably interacts in a specific fashion with that protein. This approach was first applied to crude cell extracts; the specificity of ligand-protein interactions were then further examined using purified recombinant proteins.

### **IDENTIFICATION OF PUTATIVE NUCLEOSIDE-BINDING PROTEINS: LIGAND-SPECIFIC ELUTION OF NATIVE PROTEINS BOUND TO DYE-RESIN**

When we applied a crude extract of soluble proteins from *Mycobacterium tuberculosis* (Mtb) to a column of F3GA resin, approximately 40% of the total protein remained adsorbed after extensive washing. This Mtb protein-loaded F3GA resin was used in our first ligand-specific elution screen for nucleoside/nucleotide-protein interactions, outlined in Figure 1, in which 6 to 20 potential ligands were applied successively to a given protein-loaded column, and the proteins eluted by each ligand were identified by standard proteomic tools [16]. Relatively low nucleoside concentrations (1 mM) and small volumes of eluting buffer (0.5 column bed volume) were employed, with the aim of identifying specific ligand-protein interactions.

---

Furthermore, the strong interaction of many proteins with F3GA, and the high concentration of F3GA in the resin, also served to enhance the stringency of this ligand-protein interaction assay.

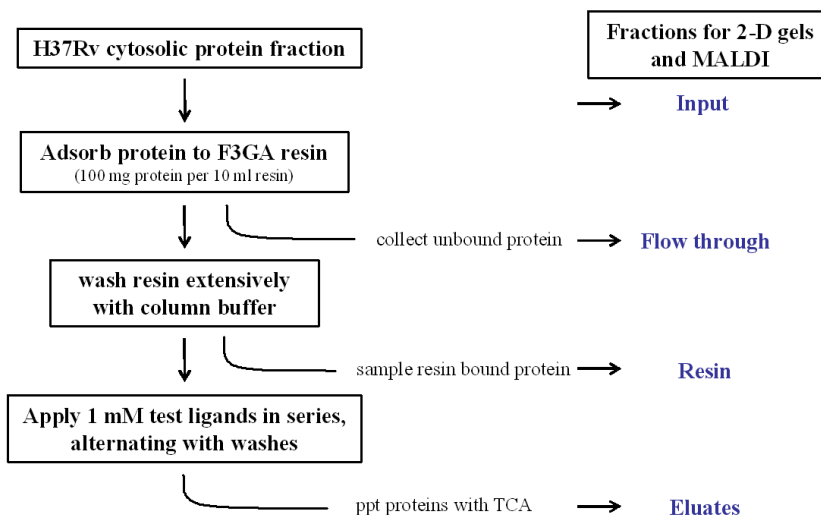


**Figure 1.** Purification of candidate nucleoside-ligand binding proteins from *M. tuberculosis* cell lysates. Affinity chromatography using immobilized Cibacron Blue F3GA was performed as outlined by Scopes [10], where Mtb proteins that bind F3GA are tested for ligand-specific elution by adding individual nucleosides or nucleotides to the column buffer. A crude cytosolic extract (100 mg) from Mtb strain H37Rv [<http://www.cvmb.colostate.edu/microbiology/tb/top.htm>] was desalted over a Sephadex G-25 column and adsorbed to a 10 ml “Affigel” Blue Gel (Cibacron F3GA Blue) (BioRad) affinity column. The affinity column was washed extensively with column buffer (CB; 50 mM  $\text{KH}_2\text{PO}_4$ , pH 7.5, 1 mM  $\text{MgCl}_2$  and 2 mM DTT) to remove unbound and low-affinity proteins prior to ligand elution. Approximately 40% of total cytosolic protein bound to the resin, as determined by Bradford assay. An aliquot of the resin-bound protein was extracted for subsequent 2D-gel analysis prior to elution (see Figure 2, top left panel); ~100 mg resin was extracted in 250  $\mu\text{l}$  urea sample buffer (USB; 8% urea, 2% NP-40, 18 mM DTT), and the solubilized protein recovered in a spin column (Costar Spin-X, cellulose acetate membrane). Ligand-specific elution was carried out using 5 ml (one half column volume) of each ligand at 1 mM in CB. Ligands were applied in series, and the column was washed with 20 ml (2 column volumes) CB between ligands. Up to 20 different ligands were used to elute proteins from a single column. Columns were monitored using an in-line flow cell at 260 nm. Peak ligand fractions were pooled and the protein precipitated by addition of 100% iced TCA to a final concentration of 20%. Precipitated proteins were recovered by centrifugation, washed with acetone, and solubilized in 300  $\mu\text{l}$  urea sample buffer. Recovered proteins were fractionated by 2-dimensional IEF-SDS-PAGE, using 13 cm pH 3–10 NL Immobilon gradient strips in the first dimension (Pharmacia Biotech IPGphor system, as per the manufacturer’s instructions), and 15% SDS slab gels in the second dimension. Proteins were stained with Coomassie Brilliant Blue R250; excised protein spots were trypsinized in situ; recovered peptides were analyzed by MALDI-TOF MS, and peptide masses were matched to predicted proteins in the Mtb genome [16].

We observed ligand-specific release of distinct assortments of individual proteins from the resin by many different ligands such as NAD and ATP (Fig. 2). Furthermore, the release of individual proteins from the Mtb protein-loaded resin was sensitive to small differences in the structure of individual ligands, such as the presence of methyl and phosphate groups on adenosine (Fig. 3).

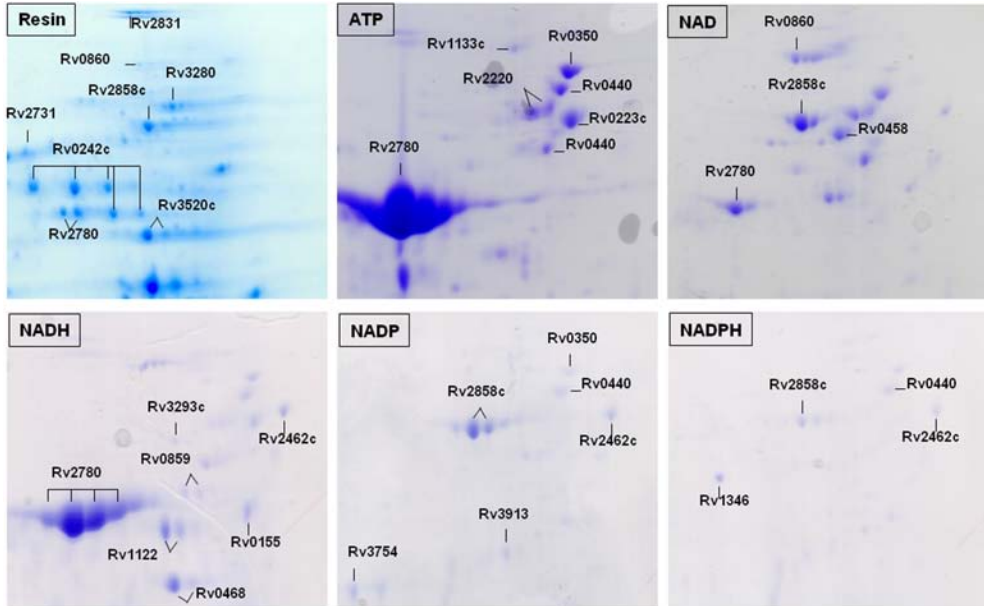


**Figure 2.** Ligand-specific elution of native Mtb proteins from Cibacron Blue F3GA resin. Two dimensional IEF-SDS-PAGE separation of Mtb cytosolic proteins that bind to the F3GA resin (top left panel), or are subsequently eluted by the indicated nucleotide at a concentration of 1 mM. Data are from three different experiments, as per figure 1. Only that portion of each gel corresponding to molecular mass ~100 to 35 kDa (top to bottom) and pI ~6 to 4.5 (left to right) is shown. Protein identities are indicated by locus tag number (see Table 1).

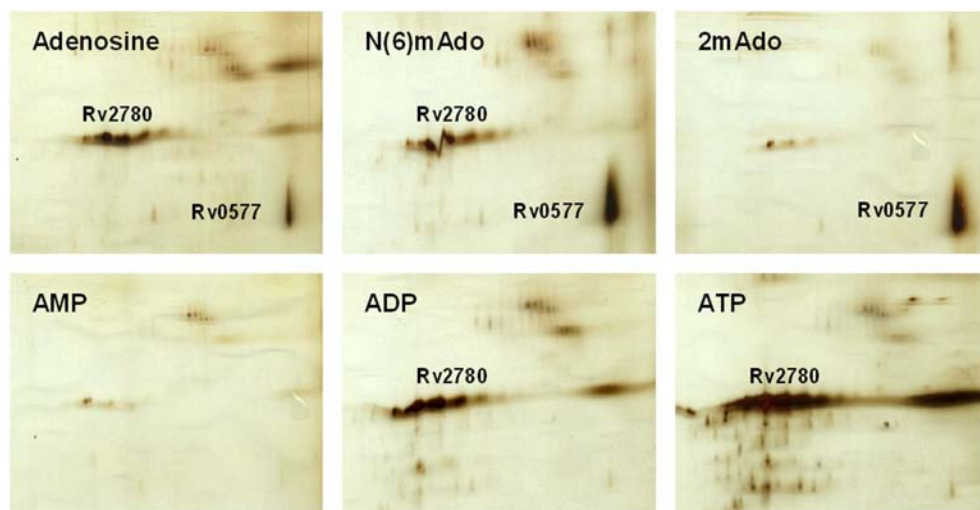


**Figure 3.** Selective elution of native Mtb proteins from F3GA resin by adenosine and adenosine analogs. Two dimensional IEF-SDS-PAGE separation of Mtb cytosolic proteins bound to F3GA and eluted successively by adenosine and related compounds. Ligands were applied to the column in the same order as the panels (from top left to bottom right, in order of increasing ligand mass), from a single experiment as per Figure 1. Rv0577 eluted with adenosine and both of the methyl-adenosine xenobiotics, but not with nucleotides. Conditions were as in Figure 2, except that proteins were stained with silver.

A summary of the predicted identities and functions (in Genbank) of the native Mtb proteins identified in different fractions described in Figure 1 are given in Tables 1 and 2. Table 1 lists 26 proteins that exhibited ligand-specific elution and in Table 3 these elution results are compared with the ligands associated with predicted protein functions available in public gene data bases. These tabulated results provide annotations of gene and predicted protein function at several levels. First, these data provide the first direct evidence that 28 Mtb proteins predicted from analysis of the Mtb genome exist *in vivo* (eight other proteins in Table 1 and 2, see footnotes). Second, the ligand-elution data provide specific annotations as to ligands that bind to these proteins. In the cases of Rv2671 and Rv3336c, for example, Table 3 shows that they bind NADPH and ATP, respectively. Table 3 contains many examples of consistency between nucleotide-elution data and the predicted ligand specificity based on gene sequence comparisons; Nineteen of the proteins in Table 3 were eluted by the predicted ligand or a very closely related one (e.g. NADP vs. NADH). Half (18/36) of the proteins identified in Tables 1 and 2 contain one or two Rossmann signatures that are associated with many nucleotide-binding proteins, including some with extensions beyond the  $GX_1-2GXXG$  core [17] sequence.

**Table 1.** Functional predictions for nucleotide-binding proteins from *M. tuberculosis* cytosolic extracts, identified by dye-ligand chromatography.

Locus tag	Protein name in GenBank	Rossmann motif
<b>Amino acid transport and metabolism</b>		
<a href="#">Rv1133c</a>	methyltransferase metE	no
<sup>a</sup> <a href="#">Rv2220</a>	glutamine synthetase glnA1	no
<sup>a</sup> <a href="#">Rv2780</a>	secreted L-alanine dehydrogenase ald	<i>VIGAGTAGYNAA</i>
<a href="#">Rv3754</a>	prephenate dehydrogenase tyrA	VLGLGLIGGSIM
<b>Carbohydrate transport and metabolism</b>		
<a href="#">Rv1023</a>	phosphopyruvate hydratase eno	STGLGDEGGFAP
<a href="#">Rv1122</a>	6-phosphogluconate dehydrogenase gnd2	MIGLGRMGANIV
<b>Lipid transport and metabolism</b>		
<a href="#">Rv0468</a>	3-hydroxybutyryl-CoA dehydrogenase fadB2	<i>VVGAGQMGSGLA</i>
<a href="#">Rv0751c</a>	3-hydroxyisobutyrate dehydrogenase mmsB	FLGLGNMGAPMS
<a href="#">Rv0824c</a>	acyl-[acyl-carrier-protein] desaturase desA1	NMGMDGAWGQWVN
<a href="#">Rv0859</a>	acetyl-CoA acetyltransferase fadA	no
<a href="#">Rv0860</a>	fatty acid oxidation protein fadB	<i>VLGAGMMGAGIA</i> <i>IVGYSGPAGTGKA</i>
<b>Nucleotide transport and metabolism</b>		
<a href="#">Rv1843c</a>	IMP dehydrogenase guaB1	AVGINGDVGAKAR
<sup>a</sup> <a href="#">Rv2445c</a>	nucleotide diphosphate kinase ndkA	no
<b>Other metabolism</b>		
<a href="#">Rv0927c</a>	short-chain dehydrogenase	no
<a href="#">Rv2671</a>	hypothetical protein, possible ribD	no
<b>Energy production and conversion</b>		
<a href="#">Rv0155</a>	NAD(P) transhydrogenase pntAa	VLGVGVAGLQAL
<a href="#">Rv0223c</a>	aldehyde dehydrogenase	no
<a href="#">Rv0458</a>	aldehyde dehydrogenase	QSGIGREGHQMM
<a href="#">Rv2858c</a>	aldehyde dehydrogenase aldC	no
<a href="#">Rv3293</a>	piperidine-6-carboxylic acid dehydrogenase pcd	no
<sup>a</sup> <a href="#">Rv3913</a>	thioredoxin reductase trxB2	<i>VIGSGPAYTAA</i>
<b>Other cellular processes</b>		
<a href="#">Rv1511</a>	GDP-D-mannose 4,6 dehydratase gmdA	<i>ITGITQDGSYLA</i>
<a href="#">Rv3336c</a>	tryptophanyl-tRNA synthetase trpS	no
<b>Poorly characterized</b>		
<a href="#">Rv0484c</a>	short-chain oxidoreductase	no
<a href="#">Rv0577</a>	hypothetical protein	no
<a href="#">Rv1544</a>	possible ketoacyl reductase	SAGFGTSGRFWE

**Locus tag** (Rv numbers) are gene identifiers for predicted open reading frames (ORFs) in the *M. tuberculosis* H37Rv genome (accessed through NCBI Entrez Gene at <http://www.ncbi.nlm.nih.gov/sites/entrez?db=gene>). For each protein recovered by dye-ligand chromatography, the masses of tryptic peptides were determined by MALDI and matched to ORFs by ProteinProspector (<http://prospector.ucsf.edu/>).

**Rossmann motif** shows which proteins contain the GX<sub>1-2</sub>GXXG core sequence characteristic of FAD, NAD(P)-binding proteins that form a Rossmann fold (BOLD), and those that also have the extended sequence shown to stabilize the fold structure (ITALIC; I or V in the 1<sup>st</sup> position shown, and A or G in the last) (Ref. 17). Note that Rv0860 contains 2 motifs.

<sup>a</sup> Indicates 4 proteins that have been previously studied (see also Table 2). The remainder are shown here, for the first time, to be expressed *in vivo*.

**Table 2.** *M. tuberculosis* proteins identified in this study for which no ligand-binding information was determined.

Locus tag	Protein name in GenBank	<sup>b</sup> Rossmann motif
<b>Lipid transport and metabolism</b>		
<a href="#">Rv0154c</a>	probable acyl-CoA dehydrogenase fadE2	no
<a href="#">Rv0242c</a>	3-ketoacyl-(acyl-carrier-protein) reductase fabG4	LVGNGSIGEGGR IAGIAGNRGQTNY
<a href="#">Rv2831</a>	enoyl-CoA hydratase echA16	no
<sup>a</sup> <a href="#">Rv3280</a>	propionyl-CoA carboxylase (beta chain 5) accD5	VMGASGAVGFVYR
<b>Energy production and conversion</b>		
<a href="#">Rv3520</a>	possible coenzyme F420-dependent oxidoreductase	ILGLGVSGPQVV LTGEGTTGLGKA
<b>Molecular chaperones</b>		
<sup>a</sup> <a href="#">Rv0350</a>	molecular chaperone DnaK	no
<sup>a</sup> <a href="#">Rv0440</a>	chaperonin groEL	VPGGGDMGGMDF
<sup>a</sup> <a href="#">Rv2031c</a>	heat shock protein hspX	no
<a href="#">Rv2462c</a>	trigger factor tig	no
<b>Poorly characterized</b>		
<a href="#">Rv2731</a>	conserved hypothetical alanine/arginine rich protein	no

Proteins listed are those which bound to the affinity resin but did not elute with any of the test ligands (e.g., see Figure 1). In addition, all of the *Molecular Chaperones* were *ubiquitous*; present at low levels in all samples, including ligand-free washes.

<sup>a, b</sup> See Table 1 footnotes. Note that Rv0242c and Rv3520 each contain 2 *Rossmann motifs*.

Some of the ligand-protein combinations identified by ligand elution are unexpected or not predicted from sequence analyses and GenBank annotations (<http://www.ncbi.nlm.nih.gov/Genbank/index.html>). For example, Rv0577 has neither a Rossmann signature, nor any GenBank annotation suggesting nucleoside-dependent function. We therefore targeted such proteins for recombinant expression to examine ligand-protein interactions under conditions where the quantities and concentration of protein are well-defined, and the effects of different ligands on protein-dye interactions can be more readily compared. The method with crude extracts, just described, is a positive screen only; proteins that elute with ligands may not be picked up due to protein abundance or detection issues, and the order of eluting ligands can influence gel spot intensity and resolution for proteins which are substantially depleted by several related ligands. Moreover, some proteins retained on the column may be bound via other proteins in native complexes, rather than directly to the dye, while other proteins may have increased or unchanged affinity for the dye when bound to ligands.

**Table 3.** Predicted ligand-protein interactions for native *M. tuberculosis* proteins versus interactions observed by dye-ligand chromatography.

Locus tag	<sup>a</sup> Predicted interactions	<sup>b</sup> Ligand[s] causing elution from F3GA resin
<a href="#">Rv0155</a>	NAD[P][H]	NADH
<a href="#">Rv0223c</a>	NAD[P][H]	ATP
<a href="#">Rv0458</a>	NAD[H]	N(6)mAdo, NAD
<a href="#">Rv0468</a>	NAD[P][H]	NADH
<a href="#">Rv0484c</a>	NAD[P][H]	NADPH
<a href="#">Rv0577</a>	na	N(6)mAdo, 2mAdo >> Ado, FAD
<a href="#">Rv0751c</a>	NAD[H]	NAD
<a href="#">Rv0824c</a>	NADPH	NADPH
<a href="#">Rv0859</a>	na	NAD[H]
<a href="#">Rv0860</a>	NAD[H]	NAD[H]
<a href="#">Rv0927c</a>	NAD[P][H]	NADP[H]
<a href="#">Rv1023</a>	na	ATP
<a href="#">Rv1122</a>	NADP[H]	NADH
<a href="#">Rv1133c</a>	na	N(6)mAdo > ATP, GTP
<a href="#">Rv1511</a>	NADP[H]	GTP
<a href="#">Rv1544</a>	NAD[P][H]	NADPH
<a href="#">Rv1843c</a>	NAD[H]	GMP
<a href="#">Rv2220</a>	ATP/ADP/AMP	2mAdo >> N(6)mAdo > ATP, FAD
<a href="#">Rv2445c</a>	NTP/NDP	ATP>GTP>>ubiquitous <sup>c</sup>
<a href="#">Rv2671</a>	NADP[H]	NADPH
<a href="#">Rv2780</a>	NAD[H]	NADH, ATP, cAMP >> ADP, Ado, N(6)mAdo
<a href="#">Rv2858c</a>	NAD[H]	NADP > NADPH, NAD
<a href="#">Rv3293</a>	NAD[P][H]	NADH
<a href="#">Rv3336c</a>	ATP/AMP	ATP
<a href="#">Rv3754</a>	NAD[H]	NADP
<a href="#">Rv3913</a>	NADP[H], FAD	NADP

<sup>a</sup> *Predicted interactions* were compiled from biochemical studies of homologous proteins in other species, available in the NCBI, Prosite and BRENDA databases, and is not available (na) for all proteins.

<sup>b</sup> *Ligands causing elution* were observed experimentally for each protein. Relative spot intensities observed on 2-D gels are indicated by rank order, and do not reflect a systematic analysis of relative ligand affinity.

<sup>c</sup> See Table 2 footnote re *ubiquitous* proteins.

## ANALYSIS OF THE SPECIFICITY OF LIGAND-PROTEIN INTERACTIONS WITH RECOMBINANT PROTEINS AND DYE-LIGAND CHROMATOGRAPHY

In the second ligand-specific elution screen for nucleoside/nucleotide-protein interactions, single recombinant Mtb proteins were adsorbed on multiple small (mg) aliquots of F3GA resin in spin columns, and assayed for elution by various nucleotides and nucleosides using one ligand per column, as outlined in Figure 4. The use of purified recombinant proteins permitted us to identify effects of a single variable (ligand structure) on the stability of the

dye-protein complexes. We found clear differences in the release of a particular protein from the affinity resin by various ligands, shown for Rv0577 in Figure 5. We posit that greater amounts of eluted protein reflect stronger interaction between the protein and eluting ligand. Here, a stronger interaction between a protein and the eluting ligand could be due either to a direct interaction of the ligand at the dye-binding site of the protein, or binding at a site remote from the dye-binding site that causes conformational changes in the protein and weakens protein-dye interactions [12]. Further, only interactions that lead to a decrease in dye-binding affinity are expected to result in elution of a protein.

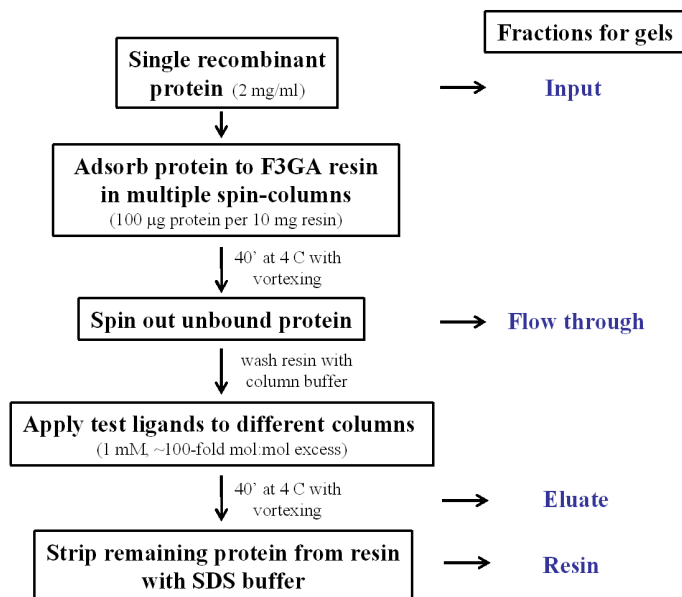


**Figure 4.** Analysis of nucleoside-ligand binding by recombinant proteins. Recombinant proteins were evaluated for their ligand-binding properties using a modified affinity elution chromatography protocol (22): individual proteins were diluted to 2 mg/ml in CB and adsorbed to multiple small aliquots of F3GA resin (100 µg protein per 10 mg resin) in 2 ml spin-columns (Costar Spin-X, cellulose acetate membrane). Binding was for 1 h at 4 °C with very gentle vortexing, followed by recovery of unbound protein (flow-through fraction) and washing of the resin (8 x 0.4 ml washes with CB); spin-columns were micro-centrifuged for 30 s at 13000 g, to recover fractions and change solutions. Individual spin-columns containing resin-bound proteins were then incubated (as for protein binding, above) with 50 µl 1 mM test ligand in CB, and the elution fractions recovered by centrifugation. Protein, which remained bound to the resin was recovered by heating at 95 °C for 5 min in 100 µl SDS sample buffer, and centrifugation (resin fraction). Aliquots of initial protein, spin-column flow-through and eluate fractions were diluted 1:1 with 2X SDS sample buffer. Equal proportions of all fractions (equivalent to 1 µg input protein) were loaded on 15% polyacrylamide one-dimensional mini-gels and stained with silver or Coomassie blue R250.

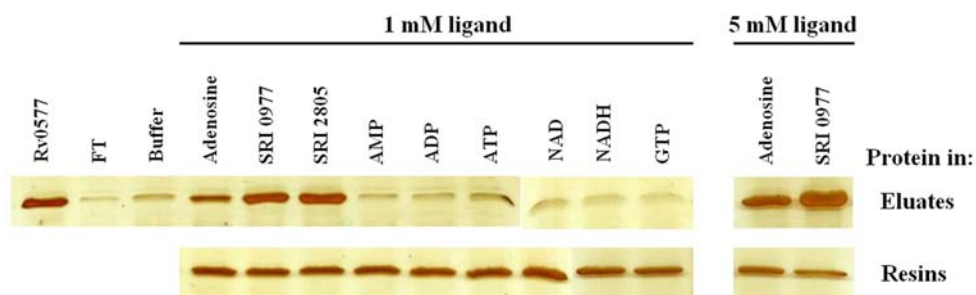


**Figure 5.** Ligand-specific elution of recombinant Mtb protein Rv0577 from Cibacron Blue F3GA resin. The protocol is described in Figure 4. Shown is the protein input (Rv0577), the protein that did not bind (FT), and the protein that was either released from F3GA resin by buffer or 9 different ligands (eluates) or remained bound to F3GA in the presence of the ligands (resins). SRI0977 = N(6)methyladenosine; SRI2085 = 2-methyladenosine. Silver staining shows release of Rv0577 from F3GA by nucleosides, but not by nucleotides.

The results with purified recombinant Mtb proteins such as Rv0577 (Fig. 5) are consistent with the observations from experiments with crude cytosolic extracts (Fig. 3; Table 3), which indicated that these proteins are nucleoside/nucleotide-binding proteins. Protein Rv0577 was eluted by the nucleoside adenosine as well as by methylated adenosine xenobiotics that are anti-Mtb drug candidates [3], whereas the common purine-containing mono- and di-nucleotides (AMP/ADP/ATP/NAD/NADH/GTP) did not promote release from the dye-resin (Fig. 5; Table 3).

## CONCLUSIONS

We conclude that the two ligand-specific elution screens described here are useful for obtaining clues about the functions of members in the important class of nucleoside-binding proteins and their parent genes. Affinity methods are often effective in picking out functional classes of proteins from complex mixtures [e.g. 18], and our first dye-based screen followed this paradigm, sorting soluble proteins from a crude cell extract according to their ability to be released from the F3GA dye by millimolar concentrations of nucleosides (Figs. 2 and 3; Table 3). In addition to uncovering the natural ligands that nucleoside/nucleotide-binding proteins can associate with in cells, the dye-based screens can be extended to identify protein targets of nucleoside-analogs of interest as potential drugs [3]. Used in tandem, the two screens allow proteins to be selected from crude cell extracts as candidate nucleoside/nucleotide-binding proteins and further examined, after cloning and expression, with respect to ligand preferences. Our results with proteins in crude extracts provided evidence that many proteins bind to multiple ligands (Table 3), findings that were confirmed in screens with pure, recombinant versions under conditions where differential release of protein from the dye resin can be assigned to differences in ligand structure (example shown in Figure 5).

The data from these combined screens are useful for confirming, refining or challenging gene annotations based on sequence analysis [e.g. 10, 11], and may also serve to complement the wealth of virtual ligand screening methodologies [19]. Furthermore, the ligand-binding data can guide protein crystallization efforts aimed at protein function via structure determination. In this context, information on ligands likely has considerable practical benefits, given that protein crystallization is often greatly improved by inclusion of ligands during crystal formation [20], and production of crystals suitable for analysis by X-ray diffraction is the principal bottleneck in structural genomics efforts today [21] (PSI target status website; [http://sg.pdb.org/target\\_centers.html](http://sg.pdb.org/target_centers.html)).

### ACKNOWLEDGEMENTS

We thank Dr. W.W.P. Chang for help developing affinity sorting methods for cell extracts; Dr. J.T. Belisle for Mtb cytosol extracts (as part of NIH, NIAID Contract No. HHSN266200400091C to Colorado State University, Fort Collins, CO); Dr. R.C. Reynolds, Southern Research Institute, Birmingham, AL, for supplying the two methylated adenosine derivatives (SRI0977 and SRI2805); N. Maes and E. Z. Alipio Lyon for technical assistance. This work was in part supported by the LANL-UCR CARE program (STB-UC:06–29) and the NIGMS Protein Structure Initiative program (NIH U54 GM074946–01).

### REFERENCES

- [1] Voet, D., and Voet, J.G. (2004) *Biochemistry*, 3rd Ed., Volume 1. J. Wiley & Sons, NJ.
  - [2] Vilchèze C, Jacobs W.R. Jr. (2007) The mechanism of isoniazid killing: clarity through the scope of genetics. *Annu. Rev. Microbiol.* **61**:35–50.
  - [3] Parker, W.B., and Long, M.C. (2007) Purine metabolism in *Mycobacterium tuberculosis* as a target for drug development. *Curr. Pharm. Des.* **13**:599–608.
  - [4] Soderling, S.H., Bayuga, S.J., and Beavo, J.A. (1999) Isolation and characterization of a dual substrate phosphodiesterase gene family: PDE10A. *Proc. Natl. Acad. Sci. U.S.A.* **96**:7071–7076.
  - [5] Joyce, M.A., Fraser, M.E., Brownie, E.R., James, M.N., Bridger, W.A., and Wolodko, W.T. (1999) Probing the nucleotide binding site of *Escherichia coli* succinyl CoA synthetase. *Biochemistry* **38**:7273–7283.
  - [6] Tsybovsky, Y., Donato, H., Krupenko, N.I., Davies, C., and Krupenko, S.A. (2007) Crystal structures of the carboxyl terminal domain of rat 10-formyltetrahydrofolate dehydrogenase: implications for the catalytic mechanism of aldehyde dehydrogenases. *Biochemistry* **46**:2917–2929.
-

- [7] Goward, C.R., and Nicholls, D.J. (1994) Malate dehydrogenase: a model for structure, evolution, and catalysis. *Protein Sci.* **3**:1883 – 1888.
- [8] Eppink, M.H., Overkamp, K.M., Schreuder, H.A., and Van Berkel, W.J. (1999) Switch of coenzyme specificity of p-hydroxybenzoate hydroxylase. *J. Mol. Biol.* **292**:87 – 96.
- [9] Wang, X., and Kemp, R.G. (1999) Identification of residues of *Escherichia coli* phosphofructo-kinase that contribute to nucleotide binding and specificity. *Biochemistry* **38**:4313 – 4318.
- [10] George, R.A., Spriggs, R.V., Bartlett, G.J., Gutteridge, A., MacArthur, M.W., Porter, C.T., Al-Lazikani, B., Thornton, J.M., and Swindells, M.B. (2005) Effective function annotation through catalytic residue conservation. *Proc. Natl. Acad. Sci. U.S.A.* **102**:12299 – 12304.
- [11] Edgar, R.C., and Batzoglou, S. (2006) Multiple sequence alignment. *Curr. Opin. Struct. Biol.* **16**:368 – 373.
- [12] Scopes, R.K. (1994) *Protein Purification: Principles and Practice*, 3rd Ed. Springer, NY.
- [13] Makara, G.M., and Athanasopoulos, J. (2005) Improving success rates for lead generation using affinity binding technologies. *Curr. Opin. Biotechnol.* **16**:666 – 673.
- [14] Erster, O., Eisenstein, M., and Liscovitch, M. (2007) Ligand interaction scan: a general method for engineering ligand-sensitive protein alleles. *Nat. Methods* **4**:393 – 395.
- [15] Turnbull, J.E., and Field, R.A. (2007) Emerging glycomics technologies. *Nat. Chem. Biol.* **3**:74 – 77.
- [16] Chang, W.W.P., Huang, L., Shen, M., Webster, C., Burlingame, A., Roberts, J.K.M. (2000) Patterns of Protein Synthesis and Tolerance of Anoxia in Root Tips of Maize Seedlings Acclimated to a Low Oxygen Environment, and Identification of Proteins by Mass Spectrometry. *Plant Physiol.* **122**:295 – 317.
- [17] Kleiger, G., and Eisenberg, D. (2002) GXXXG and GXXXA motifs stabilize FAD and NAD(P)-binding Rossmann folds through C $\alpha$ -H $\cdots$ O hydrogen bonds and van der Waals interactions. *J. Mol. Biol.* **323**:69 – 76.
- [18] Bieber, A.L., Tubbs, K.A., and Nelson, R.W. (2004) Metal ligand affinity pipettes and bioreactive alkaline phosphatase probes: tools for characterization of phosphorylated proteins and peptides. *Mol. Cell. Proteomics* **3**:266 – 72.
-

- [19] Villoutreix, B.O., Renault, N., Lagorce, D., Sperandio, O., Montes, M., and Miteva, M.A. (2007) Free resources to assist structure-based virtual ligand screening experiments. *Curr. Protein Pept. Sci.* **8**:381 – 411.
- [20] Vedadi, M., Niesen, F.H., Allali-Hassani, A., Fedorov, O.Y., Finerty, J.P.J., Wasney, G.A., Yeung, R., Arrowsmith, C., Ball, L.J., Berglund, H., Hui, R., Marsden, B.D., Nordlund, P., Sundstrom, M., Weigelt, J., and Edwards, A.M. (2006) Chemical screening methods to identify ligands that promote protein stability, protein crystallization, and structure determination. *Proc. Natl. Acad. Sci. U.S.A.* **103**:15835 – 15840.
- [21] Goh, C.-S., Lan, N., Douglas, S.M., Wu, B., Echols, N., Smith, A., Milburn, D., Montelione, G.T., Zhao, H., and Gerstein, M. (2004) Mining the structural genomics pipeline: Identification of protein properties that affect high-throughput experimental analysis. *J. Mol. Biol.* **336**:115 – 130.
- [22] Kim, C.-Y., Takahashi, K., Nguyen, T.B., Roberts, J.K.M., and Webster, C. (1999) Identification of a nucleic acid binding domain in eukaryotic initiation factor eIFiso4G from wheat. *J. Biol. Chem.* **274**:10603 – 10608.
-

